Science Press

ARTICLE

Wettability of TiZrNiCu-B/Ti60 System and Its Brazing with TiBw-TC4 Composite

Hu Shengpeng[1,2],   Chen Zubin[1,2],   Lei Yuzhen[2],   Song Xiaoguo[1,2],   Kang Jiarui[2],

Cao Jian[1],   Tang Dongyan[3]

[1] State Key Laboratory of Advanced Welding and Joining, Harbin Institute of Technology, Harbin 150001, China; [2] Shandong Provincial Key Laboratory of Special Welding Technology, Harbin Institute of Technology at Weihai, Weihai 264209, China; 3 Department of Chemistry, Harbin Institute of Technology, Harbin 150001, China

Abstract: The connection between the boron content and the wettability of TiZrNiCu/Ti60 system was studied by a sessile drop method of elevating and maintaining isothermal process under vacuum, and TiBw-TC4 composite was successfully brazed to Ti60 alloy using TiZrNiCu-B filler alloy at a brazing temperature of 940 °C for 10 min. The contact angles of TiZrNiCu/Ti60 alloy substrate with the corresponding interfacial microstructure, the interfacial microstructures and shear fractures of brazed joints were studied using SEM, EDS and XRD, and the influence of B content on interfacial microstructure and joining properties was also investigated. The results show that the added B element can react with Ti to in-situ synthesize TiB whiskers (TiBw), which results in a relative refinement of microstructure. And when the content of B is 0.3 wt%, the maximum shear strength of TiBw-TC4/TiZrNiCu-B/Ti60 joint is 177 MPa, which is 65% higher than that of the joints brazed without B. However, the excessive B worsens the wetting behavior of TiZrNiCu-B on Ti60 alloy substrate, resulting in the microvoids and disconnected areas in the brazed joint, and the shear strength decreases inevitably.

Key words: wetting; TiZrNiCu-B filler; Ti60 alloy; TiBw-TC4 composite; joint strength

Titanium alloy, which possesses desirable performance characteristics such as low density, high specific strength and excellent corrosion resistance, has a significant potential for many structural areas[1-3]. As a near-α type titanium alloy, the high-temperature Ti60 alloy with an optimized chemical structure has excellent mechanical and physical properties, which makes it possible to increase the service temperature of the components up to 600 °C, and which has been considered as a candidate material for high temperature application to fabricate aero-engine parts[4-6]. In order to expand the applications of Ti60 alloy in the engine manufacturing technical field, reliable methods and techniques for joining Ti60 alloy to metals, composites or ceramics are necessary.

There are various methods for joining alloys, composites or ceramics, of which brazing has been considered as the most effective method due to its relative simplicity, versatility and cost-effectiveness[7, 8]. In recent years, various filler metals, such as the Ag-based, are used to braze titanium alloys or TiAl alloys to ceramics or composites[9,10], especially Ag-Cu-Ti active filler metal which is widely used because the active element Ti can react with ceramic or composite to form a metal-like sub-layer between the ceramic or composite substrate and filler, which can improve the wettability of molten filler on the surface of ceramics or composites, as reviewed in many articles [11-13]. Ag-based filler possesses a great advantage to join ceramics, composites and titanium alloy, but its high cost has led many researchers to focus on Ti-based filler. For example, Song et al[14] have brazed C/C composites and Ti6Al4V using mul-

tiwall carbon nanotube reinforced TiCuZrNi brazing alloy, and the in-situ formed TiC particles induced the reinforced effects such as crack deflection, interface debonding and particle fracture. Pang et al[15] have used a multi-component TiZr-based amorphous brazing filler metal to join high-strength titanium alloy, and the result showed that the amount of intermetallics in the braze zone is reduced due to the low contents of Cu and Ni in the brazing filler metal, and high shear strength joint of ~413 MPa was obtained. Li et al [16,17] successfully boned TiC cermet to stainless steel using Ti-Nb based interlayer. He et al [18] brazed Ti3Al-base alloy with TiZrNiCu filler metal. Meanwhile, our group have used TiNi-V filler metals to braze different TiAl alloys, and reliable joints can be obtained[19]. Recently, some researchers[11,20-24] also added powders, such as C, B or TiB$_2$, into Ag-Cu-Ti filler to braze Ti alloy and C$_f$/SiC composites or ceramics, resulting in an enhanced mechanical performance due to the decrease of stress at the joint interface. Maybe, adding some powders into Ti-based brazing filler metal to form in situ particles can also reduce the brazed joint stress. It is well known that the wettability of the filler on the substrate surface is very vital for brazing, which greatly influences the performance of the joint. However, few papers have concentrated on effect of added element content in Ti-based filler metal on the wetting and brazing performance of Ti alloy substrate.

In this work, element B was added into TiZrNiCu brazing alloy, and the wettability of TiZrNiCu-B alloy with various B contents on Ti60 alloy during elevating and isothermal processes was investigated. The contact angle of molten fillers with different B contents and the corresponding interfacial microstructures were analyzed. In addition, the joining of TiBw-TC4/TiZrNiCu-B/Ti60 was carried out,

and the influence of B content on the interfacial microstructure and shear strength of brazed joints was investigated in detail.

1 Experiment

Ti60 alloy used in this study was provided by Northwest Institute for Non-ferrous Metal Research, Xi'an, China. And the Ti60 based alloy consists of ($\alpha+\beta$) duplex-phase microstructure. The dimensions of Ti60 alloy used for the wetting experiments and brazing experiments were 25 mm × 25 mm × 3 mm and 20 mm × 10 mm × 3 mm, respectively. TiBw-TC4 composite used in this study was fabricated by in-situ synthesizing TiB whisker (TiBw) reinforcement in TC4 base material, which was used for brazing experiments with the dimension of 5 mm × 5 mm × 5 mm. The wetting powders TiZrNiCu-x%B (wt%) were prepared by Ti-33.1wt%Zr- 13.4wt%Ni-13.7wt%Cu powder (≥99 wt%), B powder (≥99 wt%) and some acetone via ball-milling with a rotate speed of 200 r/min for 8 h. The morphologies and XRD pattern of TiZrNiCu-B composite filler with different B contents are shown in Fig.1 and Fig.2, respectively. Original TiZrNiCu filler is spherical, which is crushed into the rough block-shape in TiZrNiCu-B filler due to mechanical milling. It can be seen from Fig.2 that the B peak appears when adding B powder in the filler, which shows that two kinds of powders are mixed evenly that do not react with each other during the milling process. Mixed powders were cold pressed into a cylinder with a dimension of Φ3 mm × 4 mm, and then ground to a dimension of about 2 mm × 2 mm × 2 mm with a mass of about 50 mg for wetting experiments. The surface of all materials were ground with silicon carbide paper and then ultrasonically cleaned for 15 min in acetone and dried in air.
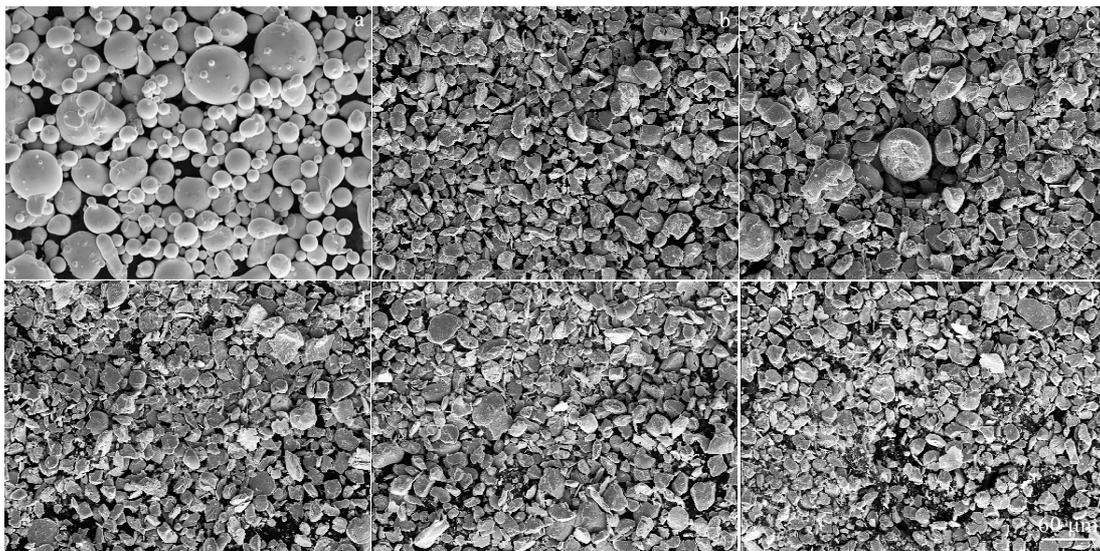
Fig.1　Morphologies of TiZrNiCu composite fillers with different B contents: (a) 0 wt%, (b) 0.3 wt%, (c) 0.6 wt%, (d) 1.0 wt%, (e) 1.5 wt%, and (f) 2.0 wt%

The sessile drop method was used for contact angle measurements under a vacuum smaller than 3×10^{-3} Pa. Before the wetting experiment, the filler metal was placed on the surface of Ti60 plate. The sample was heated to 700 °C at a rate of 20 °C/min for 10 min, and continued to be heated to 1020 °C at the rate of 4 °C/min for 10 min, and then cooled down to 600 °C at a rate of 5 °C/min and furnace-cooled down to room temperature finally. As for isothermal wetting experiments, the sample was heated from 200 °C to 1020 °C at a rate of 60 °C/min and kept for the required time to establish equilibrium conditions. The wetting process was photographed by a digital single lens reflex camera at a regular time interval, and at the end of the study, the droplet profiles were analyzed by drop-analysis software to calculate the contact angle.

In the brazing experiment, the Ti60 alloy sample, TiZr-NiCu-B filler (25 mg) and TiBw-TC4 composite sample were assembled into a sandwich structure and then placed into a resistance furnace. The assemblies were heated to 700 °C at the rate of 20 °C/min and kept for 10 min, and heated to 940 °C at the rate of 10 °C/min and held for 10 min consecutively, then cooled down to 600 °C at a rate of 5 °C/min and furnace-cooled down to the room temperature.

During the brazing process, the vacuum of furnace was $1.3 \sim 2.0 \times 10^{-3}$ Pa, and a pressure of 1 kPa was applied on the assembly to ensure proper contact.

The wetted and brazed specimens were cut perpendicularly to the contact interface, and then characterized by scanning electron microscopy (SEM) equipped with energy dispersive X-ray spectroscopy (EDS) at the operation voltage of 20 kV. The shear strength of brazed joints was measured at a constant speed of 0.5 mm/min by a universal testing machine. For each data, at least five samples were tested and the average value was obtained. After shear test, the fracture surfaces of brazed joints were examined by SEM with EDS and X-ray diffraction (XRD) to clarify the fracture mode and fracture locations.

2 Results and Discussion

2.1 Wetting behavior of TiZrNiCu/Ti60 system with different Boron contents

Fig.3a shows the variation in contact angle for different B contents in TiZrNiCu/Ti60 system with temperature, which proves that the content of B has a great influence on the contact angle between the melts and Ti60 alloy substrate. Firstly, the contact angle of TiZrNiCu on Ti60 alloy
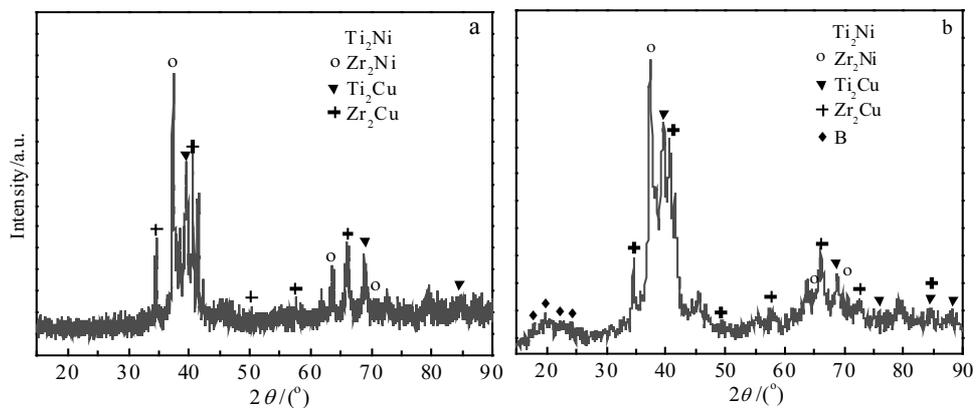
Fig.2   XRD patterns of fillers: (a) TiZrNiCu and (b) TiZrNiCu-2wt%B
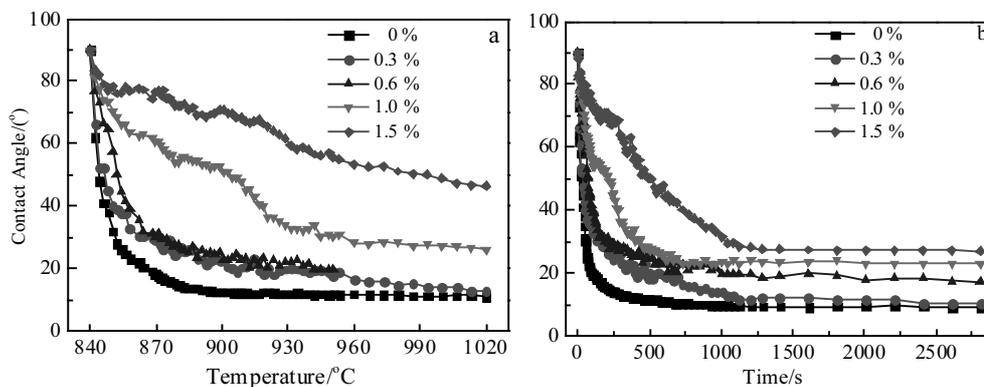
Fig.3   Variation of contact angle with temperature (a) and wetting time (b) for different B contents

substrate decreases by increasing the wetting temperature. The contact angle of ~90° indicates that TiZrNiCu-B does not be wetted on the Ti60 alloy substrate when the wetting temperature is 840 °C. As the wetting temperature increases, the contact angle decreases obviously, indicating the improved wettability. Secondly, spreading process can be divided into two stages. (1) Rapid-decrease process (840~870 °C): the contact angle decreases dramatically with increasing the wetting temperature, especially in low B content filler, such as TiZrNiCu, TiZrNiCu-0.3wt% B and 0.6 wt% B filler. (2) Slow-decrease process (870~1020 °C): as the temperature increases, the contact angle decreases slowly or even reamins constant in this process. These phenomena are consistent with the results of Fu et al[25]. The slope of the first stage decreases with the increase of B content, while increases during the second stage. Inaddtion, under the same wetting parameters, the contact angle presents an increasing trend with the rising of B content, which means the decreased wettability.

In order to further investigate the spreading of TiZrNiCu-B at a certain temperature, isothermal wetting experiments were performed at 1020 °C, and the variation of contact angle is shown in Fig.3b. Firstly, contact angle and wetting time are negatively correlated. The contact angle decreases with time, until it reaches the equilibrium or quasi-equilibrium state and no longer changes. Secondly, similar to elevating process, the spreading process can be divided into two stages: rapid-decrease process and slow-decrease process. Thirdly, the contact angle of TiZrNiCu-B on Ti60 alloy substrate increases by increasing the B content at a certain temperature for the same time.

After cooling from 1020 °C to room temperature, the macroscopic morphology of droplets with different B contents is shown in Fig.4. It is worth noting that with the increase of B content, the contact angle of composite filler increases while the spreading area decreases. As shown in Fig.4b and 4c, the droplet has a distinct spreading when the content of B is lower than 0.6 wt%, which ensures a uniform distribution of filler on the surface of Ti60 substrate. A platform presented that spreading of droplet was restricted when B content was 1.0 wt%, and the restriction was reinforced with the further increase of B content. From the investigation of Fig.3 and 4 above, it can be concluded that composite filler possesses an excellent wettability when the content of B is 0.3wt% or 0.6wt%. Increasing B content in composite filler deteriorates the wetting behavior of TiZrNiCu-B on Ti60 alloy substrate.

To further investigate the effect of increasing B content on wettability, high resolution microscopic appearance of the wetted specimens was observed by scanning electron microscope (SEM). Fig.5 shows the high resolution microscopic surface morphology of the composite fillers with different B contents after wetting. With increasing the B content, the surface topography changes as follows. Firstly, the grain size of re-solidified composite filler is gradually reduced. Secondly, less surface microvoids can be found when the content of B is lower than 0.6 wt%, but the surface microvoids dramatically increase when B content is more than 1.0 wt%, as shown in Fig.5d and 5e.

Fig.6 shows the highly magnified SEM images of surface morphology of wetted samples with 0.6 wt% and 1.5 wt% B content. Some TiB whiskers can be found, and the quantity of whiskers increased when the B content increased from 0.6 wt% to 1.5 wt%. According to the Ti-B binary phase diagram[26], Ti reacts with B to form TiB and TiB2, the reactions are shown in Eq.(1), (2) and (3) [27], and the curves of Gibbs free energy ΔG of the three reactions vary with
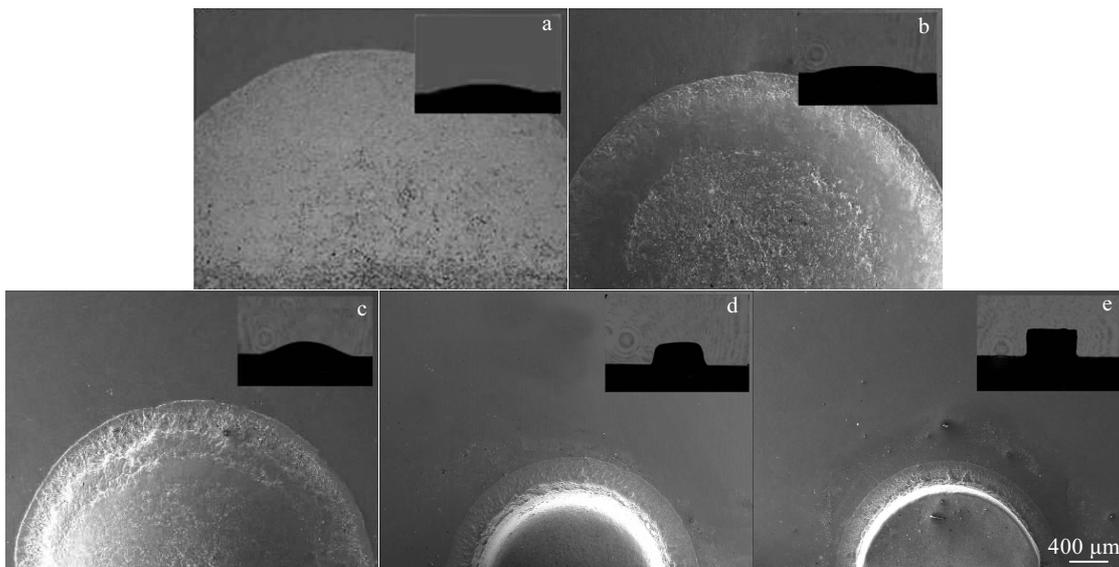
Fig.4   Macrographs of droplet with different B contents: (a) 0 wt%, (b) 0.3 wt%, (c) 0.6 wt%, (d) 1.0 wt%, and (e) 1.5 wt%
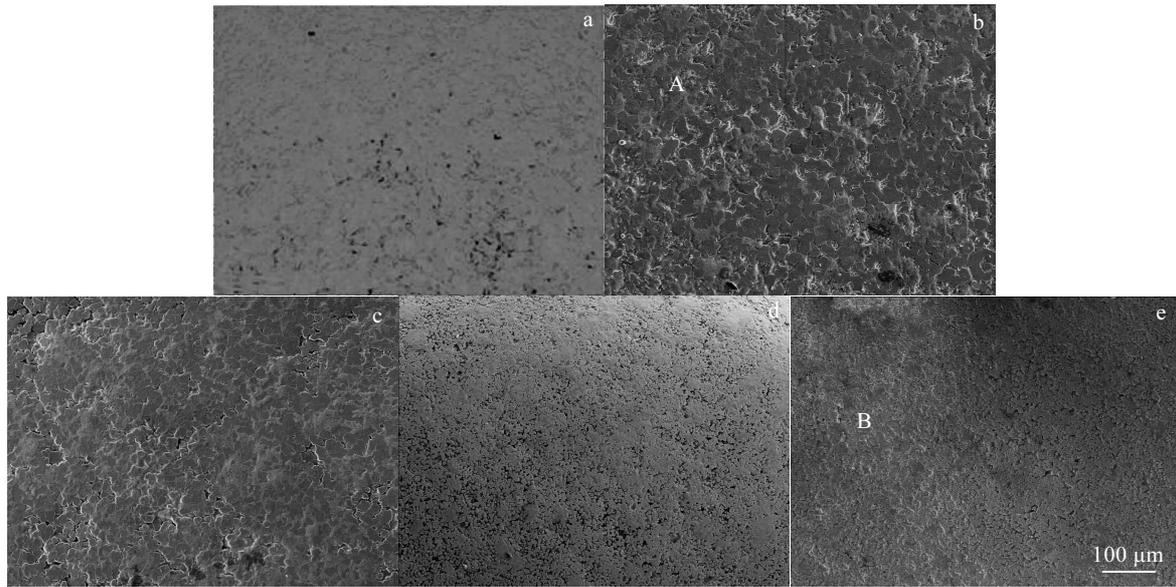
Fig.5   Surface morphologies of wetted samples with different B contents: (a) 0 wt%, (b) 0.3 wt%, (c) 0.6 wt%, (d) 1.0 wt%, and (e) 1.5 wt%
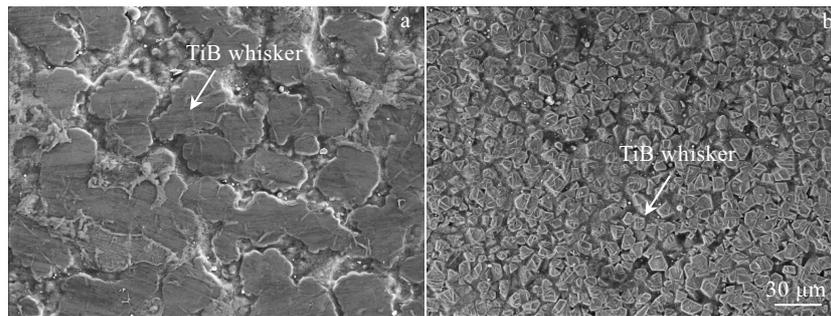
Fig.6   Magnified SEM images of TiB whisker of zone A in Fig.5b (a) and zone B in Fig.5e (b)

temperature[27], as shown in Fig.7. ΔG of all the three reactions is negative in the range of 500 ~1020 °C, indicating that the reaction can spontaneously occur in the wetting process. As shown in Fig.7, it can be concluded that the Gibbs free energy of TiB_2 is much lower than that of TiB during the wetting process, so Ti reacts with B following the Eq.(2) to form TiB_2 at first, and then $TiB_2+Ti\rightarrow2TiB$ occurs. But Fig.6 shows no bulk TiB_2 phases, which can also be proved by XRD patterns in Fig.13. According to the study of Fan et al[28], the growth rate of the TiB whiskers in the needle-like direction was nearly six times larger than that of the bulk TiB_2, the dissolution coefficient of B in the needle-like direction of the TiB was much larger than that of the TiB_2, and the activation energy of B in the two phases was almost the same, which indicates that the TiB phase is more thermodynamically stable than TiB_2. When sufficient Ti element can be provided for the reaction

Ti+B→TiB during the wetting process, TiB_2 will only act as a transition phase and will only appear if the Ti element is consumed.

$$Ti+B\rightarrow TiB \tag{1}$$
$$Ti+2B\rightarrow TiB_2 \tag{2}$$
$$Ti+TiB_2\rightarrow 2TiB \tag{3}$$

The backscattered electron (BSE) images in Fig.8 display the interfacial microstructures of droplets on Ti60 alloy substrate with different B contents. It can be seen that all the samples contained a thick diffusion layer between filler and substrate. The thickness of diffusion zone increases when the content of B rises to 0.6 wt%, and the thickness of the diffusion layer of 0.6 wt% B presents the highest value of about 150 μm. When the B content further increases, the thickness of diffusion zone has a gradual reduction. Furthermore, fewer microvoids can be found when B is added, which is consistent with the results and discussion of Fig.5 above.
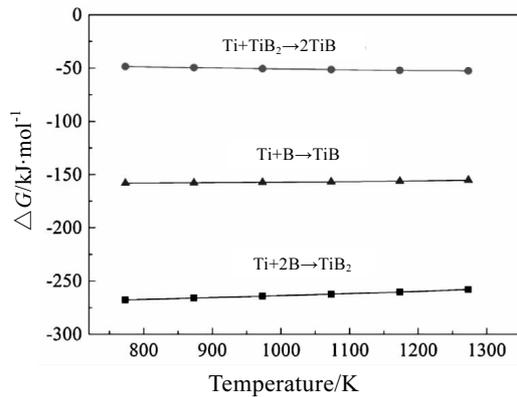
Fig.7 Gibbs free energy curves of Ti-B reaction [27]

According to the EDS results in Table.1, the main chemical elements are Ti, Zr, Ni and Cu. Some articles showed that the Zr element can be dissolved in Ti_2Ni and Ti_2Cu compounds[29-33]. The bright white phase may be Ti_2Ni, Ti_2Cu, Zr_2Ni and Zr_2Cu, which can be summarized as (Ti, Zr)$_2$(Ni, Cu) intermetallic compounds[34]. According to relevant literatures[35-38], only considering the thermodynamic information, the Gibbs free energies for forming these Ti_2Ni, Ti_2Cu, Zr_2Ni and Zr_2Cu were negative under equilibrium when the wetting temperature was 840~1020 °C. Therefore, the formation of (Ti,Zr)$_2$(Ni,Cu) intermetallic compounds is possible, as shown in Eq. (4)~(7).

$$\Delta G_f^0 \ (Ti_2Ni) = -73.900 - 0.045T \ (kJ/mol) \tag{4}$$

$$\Delta G_f^0 \ (Ti_2Cu) = -24.220 + 0.0085T \ (kJ/mol) \tag{5}$$

$$\Delta G_f^0 \ (Zr_2Cu) = -84.379 + 0.000325T \ (kJ/mol) \tag{6}$$
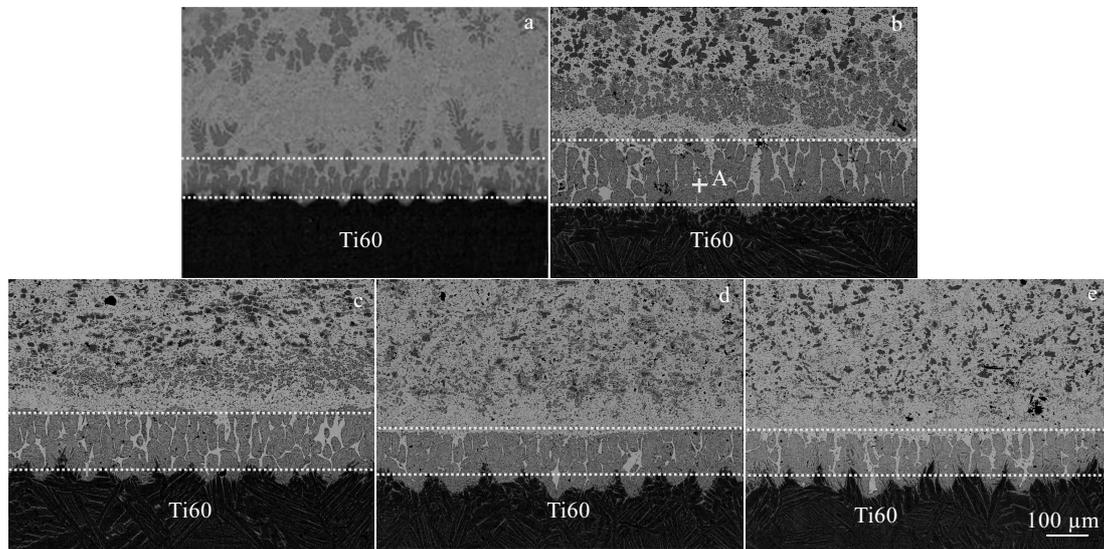
Fig.8 Microstructures of droplet/Ti60 interface with different B contents: (a) 0 wt%, (b) 0.3 wt%, (c) 0.6 wt%, (d) 1.0 wt%, (e) and 1.5 wt%

Table 1 EDS results of zone A marked in Fig.8b (at%)

Ti	Zr	Ni	Cu	Possible phase
88.7	3.9	4.3	3.1	β-Ti+(Ti, Zr)$_2$(Ni, Cu)

$$\Delta G_f^0 \ (Zr_2Ni) = -187.645 - 0.013626T \ (kJ/mol) \tag{7}$$

The light gray area near the Ti60 alloy side, which is mainly composed of Ti elements and a small amount of Zr, Ni and Cu elements, may be Ti-based solid solution. Element Ni and Cu are β-phase stable elements in Ti alloy, which can promote the transformation of β phase. From the discussion above, it can be inferred that the diffusion layer mainly consists of light gray β-Ti and bright white compound (Ti,Zr)$_2$(Ni,Cu), and XRD patterns in Fig.13 can also prove it.

Fig.9 shows the magnified SEM image of droplet/Ti60 interface. With the increase of the content of B, large num-

bers of TiBw precipitated on the bright white phase, and the original continuous black phase and white phase transformed into discontinuities. It can be conjectured that the microstructure can be refined by whisker.

The effect of B content on wetting behavior of TiZrNiCu/Ti60 system can be summarized as follows. Firstly, boron can react with titanium to in-situ synthesize TiB whiskers (TiBw) during the wetting process. The high hardness of TiBw can prevent the grain boundary migration and inhibit grain growth, so as to control the grain size and the grains become fine, as illustrated in Fig.5 and 9. But excessive B would lead to a large amount of TiBw and whisker structures, which resulted in a reduction of capillary action of the liquid filler and emergence of microvoids, as shown in Fig.5, 7, 8 and 9. Secondly, the added micron B powder, due to its fine particle size, high hardness and high melting point, can be regarded as the second phase in the

molten filler. The B addition with higher surface energy, compared to the molten TiZrNiCu filler, will increase the viscosity of filler, thereby reducing the fluidity of filler. Thirdly, with the increase of B content, more in-situ spontaneous reaction Ti+B→TiB occurs, which consumes more Ti active element and results in a decrease in wettability during wetting process. Finally, the formation of large amounts of TiB whiskers increases the nucleation sites; newly-born phases precipitate closely around the TiB whisker, which further reduces the content of filler to wet the substrate. Therefore, the wettability of TiZrNiCu-B on Ti60 alloy substrate with high B content is decreased.

2.2 Effect of B content on TiBw-TC4/TiZrNiCu/ Ti60 brazed joint

Fig.10 shows the microstructure evolution in backscattered electron (BSE) mode and the EDS results of the TiBw-TC4/TiZrNiCu-B/Ti60 joints brazed with different B contents at 940 °C for 10 min. The joint classified by morphology consisted mainly of three characteristic zones: zone Ⅰ (diffusion zone adjacent to TiBw-TC4), zone Ⅱ (brazing seam) and zone Ⅲ (diffusion zone adjacent to Ti60). From Fig.10a and discussion above, it can be con-

cluded the interfacial microstructure of joint brazed with TiZrNiCu-B filler is TiBw-TC4/α-Ti+ β-Ti+(Ti,Zr)$_2$(Ni,Cu)/ (Ti,Zr)$_2$(Ni,Cu)+TiBw/α-Ti+β-Ti+(Ti,Zr)$_2$(Ni,Cu)/Ti60.As B content rises, the number of in-situ synthesized TiBw increased, and (Ti,Zr)$_2$(Ni,Cu) in the braze seam became more dispersive, and moreover, the microstructure got refined due to the existence of TiBw, especially when the B content is 2.0 wt%, as shown in Fig.10e. Excessive B may lead to a large amount of TiBw, which brought about microvoids and disconnected area in the joint, as revealed in Fig.10e. This is also consistent with the analysis of section 2.1 above.

The evolution of interfacial microstructure plays an important role in determining shear strength of brazed joints. Fig.11 shows the room-temperature shear strength of the joint brazed with composite filler added with different B contents at 940 °C for 10 min. The result revealed that the shear strength of the joints firstly increases and then decreases with the increase of B content. The maximum shear strength of 177 MPa is obtained when the B content is 0.3 wt%, which is 65% higher than that of the joint brazed without B.
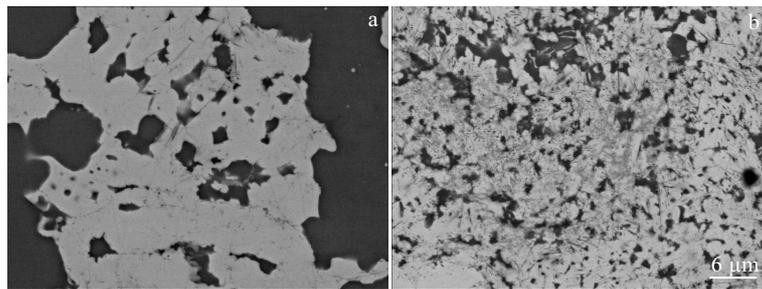
Fig.9   Magnified SEM image of droplet/Ti60 interface: (a) 0.3 wt% and (b) 1.5 wt%
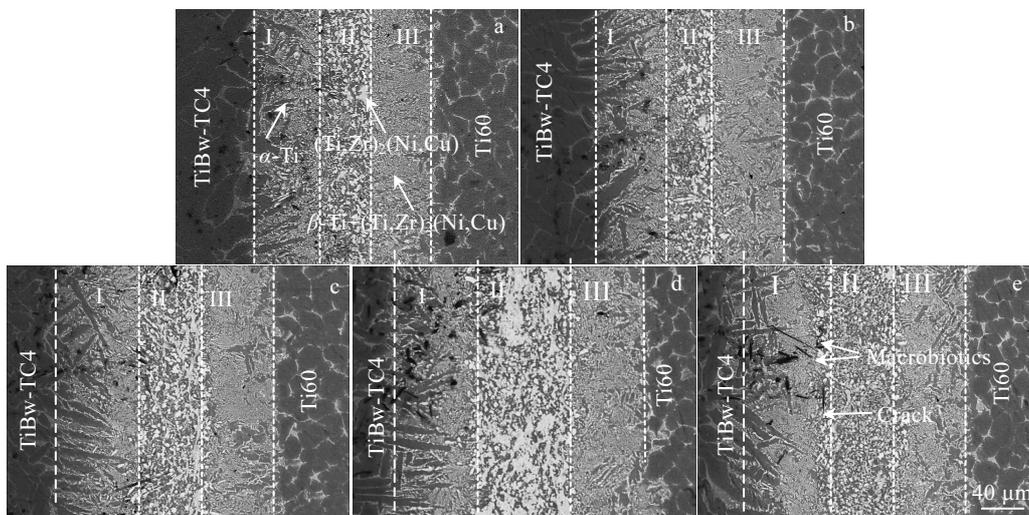
Fig.10   Microstructures of TiBw-TC4/TiZrNiCu/Ti60 brazed joints with different B contents at 940 °C for 10 min: (a) 0 wt%, (b) 0.3 wt%, (c) 0.6 wt%, (d) 1 wt%, and (e) 2.0 wt%
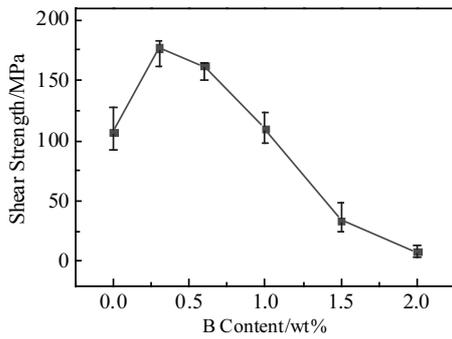
Fig.11   Effect of B content on shear strength of TiBw-TC4/TiZr
NiCu/Ti60 brazed joint

To realize the fracture behavior of brazed joint, the fracture surface was observed by SEM with EDS and analyzed by XRD after the shear test, and the results are shown in Fig.12, Table 2 and Fig.13. Fig.12a shows that the fracture surface of a specimen brazed with single TiZrNiCu filler is relatively flat and smooth, and EDS result in Table 2 shows that $(Ti,Zr)_2(Ni,Cu)$ exists on fracture surface, which indicates the cleavage topography surface and the brittle mode (Fig.12b). For the joint with 0.3 wt% B, the fracture surface is uneven, indicating that the fracture path is not broken along a certain plane, as shown in Fig.12c. In Fig.12d, combined with XRD pattern and EDS result, it can be concluded that some $(Ti,Zr)_2(Ni,Cu)$ zones (marked as B), β-Ti+$(Ti,Zr)_2(Ni,Cu)$ zones (marked as C)+α-Ti zones (marked as D) and TiB whiskers appear at fracture surface,
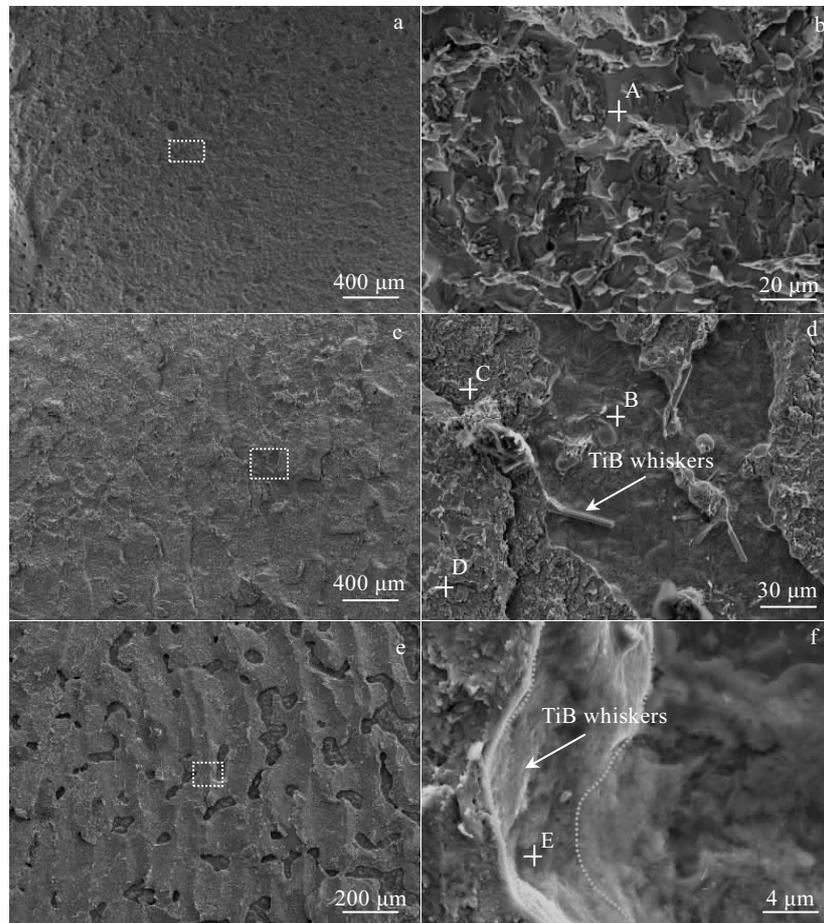
Fig.12   SEM fracture morphologies of Ti60/TiBw-TC4 brazed joints with different B contents after shear test on TiBw-TC4 side: (a, b) 0
wt%, (c, d) 0.3 wt%, and (e, f) 2.0 wt%

which indicates that the fracture partially occurs in the intermetallic compound zone of brazing seam and the other occurs in diffusion layer adjacent to Ti60, and   the mode is quasi-cleavage fracture. Compared with the joint with 0.3 wt% B, the fracture of the 2.0 wt% B joint in Fig.12e is smoother and flatter. The phase of flat plane is α-Ti+β-Ti, and large numbers

numbers of scallops composed of intermetallic compounds are found. As revealed in Fig.12f, a large number of TiB whiskers exist on the fracture surface, which is confirmed by XRD pattern in Fig.13b. It can be inferred that the fracture occurs in the area between brazing seam and diffusion layer adjacent to Ti60, and has brittle characteristics.

Table 2   EDS results of each spot marked in Fig.12 (at%)

Spot	Ti	Zr	Ni	Al	Cu	Sn	B	Possible phase
A	39.6	22.4	13.6	9.7	14.7	-	-	$(Ti,Zr)_2(Ni,Cu)$
B	42.7	19.4	13.9	8.6	15.4	-	-	$(Ti,Zr)_2(Ni,Cu)$
C	64.2	13.4	6.7	7.1	8.6	-	-	β-Ti+$(Ti,Zr)_2(Ni,Cu)$
D	89.1	4.9	-	4.9	-	1.1	-	α-Ti
E	28.5	6.8	4.7	3.2	4.9	-	51.9	TiB+$(Ti,Zr)_2(Ni,Cu)$
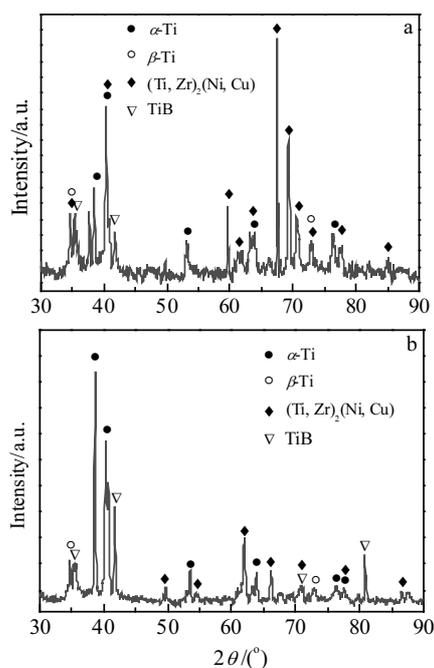
Fig.13   XRD patterns of Ti60/TiBw-TC4 brazed joints with different B contents after shear test: (a) 0.3 wt% and (b) 2.0 wt%

When the 0.3 wt% B was added into the TiZrNiCu filler, in-situ synthesized TiB whiskers could refine the microstructure in the joint, and the fraction of intermetallic compounds in the brazing seam was reduced through the Ti element consumed by element B, which causes a great improvement in the shear strength of the joints. However, with further increase of B content, excessive in-situ synthesized TiB whiskers may form whisker structures and could act as nucleation sites, resulting in the accumulation of compounds, which may reduce the wettability of the filler, and which can generate some microvoids in the joint; thus the shear strength decreases. Therefore, only appropriate B content in the filler metal can have a positive effect on the brazing properties.

3   Conclusions

1) TiBw-TC4 composite is successfully brazed to Ti60 alloy using TiZrNiCu-B filler alloy at a brazing temperature of 940 °C for 10 min.

2) The added B can react with titanium to in-situ synthe-

size TiB whiskers (TiB$_w$) in the wetting experiment, which results in a relative refinement of microstructure. The composite filler possesses a relatively excellent wettability when the content of B is 0.3 wt% or 0.6 wt%, and the further increase of B content in composite filler worsens the wetting behavior of TiZrNiCu-B on Ti60 alloy substrate.

3) The maximum shear strength of TiBw-TC4/TiZrNiCu-B/Ti60 joint is 177 MPa when B content is 0.3 wt% and it is brazed at 940 °C for 10 min, which is 65% higher than that of the joints brazed without B.

References

1 Poorganji B, Yamaguchi M, Itsumi Y *et al. Scripta Materialia*[J], 2009, 61(4): 419

2 Weiss I, Froes F H, Eylon D *et al. Metallurgical Transactions A*[J], 1986, 17(11): 1935

3 Weiss I, Semiatin S L. *Materials Science & Engineering A*[J], 1999, 263(2): 243

4 Jia W, Zeng W, Liu J *et al. Materials Science & Engineering A*[J], 2011, 530(1): 511

5 Huang L J, Yang F Y, Hu H T *et al. Materials & Design*[J], 2013, 51(5): 421

6 Zhao Z L, Li H, Fu M W *et al. Journal of Alloys & Compounds*[J], 2014, 617: 525

7 Koltsov A, Hodaj F, Eustathopoulos N *et al. Scripta Materialia*[J], 2003, 48(4): 351

8 Xue X M, Wang, J T, Sui Z T. *Journal of Materials Science*[J], 1993, 28(5): 1317

9 Wang N, Wang D P, Yang Z W *et al. Ceramics International*[J], 2016, 42(11): 12 815

10 Dai X Y, Cao J, Liu J K *et al. Materials & Design*[J], 2015, 87: 53

11 Niu G B, Wang D P, Yang Z W *et al. Ceramics International*[J], 2017, 43(1): 439

12 Xiong J H, Huang J H, Zhang H *et al. Materials Science & Engineering A*[J], 2010, 527(4-5): 1096

13 Liu D, Niu H W, Liu J H *et al. Materials Characterization*[J], 2016, 120: 249

14 Song X R, Li H J, Zeng X. *Journal of Alloys & Compounds*[J], 2016, 664: 175

15 Pang S, Sun L, Xiong H *et al. Scripta Materialia*[J], 2016, 117: 55

16 Li J, Sheng G M. *Rare Metal Materials & Engineering*[J], 2017, 46(4): 882

17 Li J, Sheng G, Li H *et al. Rare Metal Materials & Engineering*[J], 2016, 45(3): 555

18 He P, Feng J C, Zhou H. *Materials Science and Engineering A*[J], 2005, 392: 81

19 Song X G, Cao J, Chen H Y *et al. Materials Science & Engineering A*[J], 2012, 551(8): 133

20 Qiu Q, Wang Y, Yang Z *et al. Journal of the European Ceramic Society*[J], 2016, 36(8): 2067

21 Lin G B, Huang J H, Zhang H. *Materials Transactions*[J],

2006, 47(4): 1261

22　Yang M X, Lin T S, He P *et al. Materials Science and Engineering A*[J], 2011, 528: 3520

23　Yang M X, Lin T S, He P *et al. Ceramics International*[J], 2011, 37: 3029

24　Yang M X, He P, Lin T S. *Journal of Materials Science and Technology*[J], 2013, 29(10): 961

25　Fu W, Song X G, Zhao Y X *et al. Materials & Design*[J], 2017, 115: 1

26　Massalski T B, Murray J L, Bennett L H *et al. Binary Alloy Phase Diagrams*[M]. Ohio: Am Soc Met Metals Park, 1986

27　Panda K B, Chandran K S R. *Metallurgical & Materials Transactions A*[J], 2003, 34(6): 1371

28　Fan Z, Guo Z X, Cantor B. *Composites Part A Applied Science & Manufacturing*[J], 1997, 28(2): 131

29　Effenberg G, Ilyenko S eds. *Non-ferrous Metal Systems*. *Part 3, Cu-Ti-Zr* (*Copper-Titanium-Zirconium*)[M]. Berlin Heidelberg: Springer, 2007: 436

30　Balcerzak M. *Journal of Alloys and Compounds*[J], 2016, 658: 576

31　Zavaliy I, Wojcik G, Mlynarek G *et al. Journal of Alloys & Compounds*[J], 2001, 314(1-2): 124

32　Kocjan A, J Mcguiness P, Kobe S. *International Journal of Hydrogen Energy*[J], 2010, 35(1): 259

33　Chang C T, Wu Z Y, Shiue R K *et al. Materials Letters*[J], 2007, 61(3): 842

34　Lee M K, Kim K H, Lee J G *et al. Materials Characterization*[J], 2013, 80(6): 98

35　Cacciamani G, Riani P, Valenza F. *Calphad*[J], 2011, 35(4): 601

36　Turchanin M A, Agraval P G, Abdulov A R. *Powder Metallurgy & Metal Ceramics*[J], 2008, 47(5-6): 344

37　Wang N, Li C, Du Z *et al. Calphad*[J], 2006, 30(4): 461

38　Wang N, Li C, Du Z *et al. Calphad*[J], 2007, 31(4): 413

TiZrNiCu-B/Ti60 润湿性及其与 TiBw-TC4 钎焊研究

胡胜鹏 [1,2]，陈祖斌 [1,2]，雷玉珍 [2]，宋晓国 [1,2]，康佳睿 [2]，曹　健 [1]，唐冬雁 [3]

(1. 哈尔滨工业大学　先进焊接与连接国家重点实验室，黑龙江　哈尔滨　150001)

(2. 哈尔滨工业大学（威海）　山东省特种焊接技术重点实验室，山东　威海　264209)

(3. 哈尔滨工业大学　化学系，黑龙江　哈尔滨　150001)

摘　要：采用座滴法在真空下研究了硼含量对 TiZrNiCu/Ti60 润湿性的影响，且在 940 ℃保温 10 min 条件下实现了其与 TiBw-TC4 的钎焊。通过 SEM、XRD 以及剪切实验研究了界面显微组织及剪切力学性能。结果表明，添加 B 元素可以与 Ti 原位合成 TiBw，从而细化界面的显微组织。当 B 质量分数为 0.3%时，TiBw-TC4/TiZrNiCu-B/Ti60 接头的最大抗剪切强度为 177 MPa，比无 B 的接头强度高 65%。然而，过量的 B 含量使 TiZrNiCu-B 在 Ti60 合金基体上产生大量的 TiBw，导致润湿性恶化，在钎焊接头形成微孔和未焊合区域，从而使抗剪切强度下降。

关键词：润湿；TiZrNiCu-B钎料；Ti60合金；TiB$_w$-TC4复合材料；接头性能

作者简介：胡胜鹏，男，1987 年生，博士，哈尔滨工业大学先进焊接与连接国家重点实验室，黑龙江　哈尔滨　150001，电话：0631-5678454，E-mail: husp@hitwh.edu.cn